J Neuropathol Exp Neurol
Vol. 78, No. 1, January 2019, pp. 3–9
doi: 10.1093/jnen/nly105

BRIEF REPORT

Severe *TUBB4A*-Related Hypomyelination With Atrophy of the Basal Ganglia and Cerebellum: Novel Neuropathological Findings

Kristina M. Joyal, MD, Jean Michaud, MD, FRCPC, Marjo S. van der Knaap, MD, PhD, Marianna Bugiani, MD, PhD, and Sunita Venkateswaran, MD, FRCPC

Abstract

Hypomyelination with atrophy of the basal ganglia and cerebellum (H-ABC) is a rare hypomyelinating leukodystrophy characterized by infantile or childhood onset of motor developmental delay, progressive rigidity and spasticity, with hypomyelination and progressive atrophy of the basal ganglia and cerebellum due to a genetic mutation of the *TUBB4A* gene. It has only been recognized since 2002 and the full spectrum of the disorder is still being delineated. Here, we review a case report of a severely affected girl with a thorough neuropathological evaluation demonstrating novel clinical and pathological findings. Clinically, our patient demonstrated visual dysfunction and hypodontia in addition to the typical phenotype. Morphologically, more severe and widespread changes in the white matter were observed, including to the optic tracts; in gray structures such as the caudate nucleus, thalamus, globus pallidus, and substantia nigra; as well as an area of focal cortical dysplasia. Overall this case offers further insight into the broad range of clinical and neuropathological findings that may be associated with H-ABC and related *TUBB4A* gene mutations.

Key Words: Hypomyelination, Hypomyelination with atrophy of the basal ganglia and cerebellum (H-ABC), Leuko-axonopathy, Leukodystrophy, *TUBB4A*.

INTRODUCTION

Hypomyelination with atrophy of the basal ganglia and cerebellum (H-ABC) is a genetic syndrome due to a dominant mutation in the *TUBB4A* gene (1,2). In a recent review with a proposed classification system, it was included in the leuko-axonopathies (1). It is a rare hypomyelinating leukodystrophy characterized by infantile or childhood onset of motor developmental delay, progressive rigidity and spasticity, with hypomyelination and progressive atrophy of the striatum and cerebellum (1,3). The phenotypic spectrum of *TUBB4A*-related leukodystrophies continues to expand. Here, we describe a severe infantile presentation of this disorder with impressive MRI and novel neuropathological findings.

CASE PRESENTATION

A six-month-old Caucasian girl first presented with an apparent life-threatening event. She was noted to have significant, progressive microcephaly: head circumference was 36 cm (75%) at birth, 37 cm (50%) at 1 month, and 38 cm (25%) at 2 months. Her head control deteriorated between 2 and 4 months of age and she had difficulty in sucking and swallowing. On examination, she was socially responsive, able to coo, but had severe head lag, axial hypotonia, spastic quadriparesis, and cortical visual impairment. She had episodes of sudden arm and leg stiffening appearing myoclonic in nature; EEG displayed diffuse background slowing and poor reactivity.

At 9 months of age she required a gastrostomy tube. Between 9 and 24 months of age, she made minimal motor gains but became more alert and interactive. Hypodontia was noted, with the eruption of 4 incisors and molars at 25 months of age. Her hair was noted to be fine and blond, and she had long curly eyelashes. She had some antigravity movements, was able to roll and bringing hands to midline at her maximal development. With time, she became more spastic and dystonic. Tonic stiffening could be triggered by loud noises and interfered with daily functions such as diaper changes. A trial of trihexiphenidyl did not improve symptoms.

At 30 months, seizures characterized by behavioral arrest, tonic posturing, abnormal eye movements, and chewing movements developed. These improved with levetiracetam. Six months later, she began having clusters of tonic spasms, especially while asleep, without EEG correlation. By 3 years of age she remained unable to hold her head up and had significant, worsening spasticity, and dystonia. There was no improvement with addition of L-dopa or clobazam. At this point, her EEG demonstrated frequent epileptiform activity from bilateral frontocentral regions increasing with sleep, with generalized background suppression. Episodes of bilateral slow arm

From the Division of Pediatric Neurology, Children's Hospital of Eastern Ontario, Ottawa, Ontario Canada (KMJ, SV). Department of Pathology and Laboratory Medicine, Children's Hospital of Eastern Ontario and University of Ottawa, Ottawa, Ontario, Canada (JM). Department of Child Neurology, Amsterdam Neuroscience, VU University Medical Center, Amsterdam, Netherlands (MSvdK). Department of Neuropathology, Amsterdam Neuroscience, VU University Medical Center, Amsterdam, Netherlands (MB).

Send correspondence to: Sunita Venkateswaran, MD, FRCPC, Division of Pediatric Neurology, Children's Hospital of Eastern Ontario, 401 Smyth Road, Ottawa, Ontario, K1H 8M8, Canada. E-mail: svenkateswaran@cheo.on.ca

extension were captured, associated with delta slowing but no clear epileptiform activity. She continued to decline and passed away at the age of 3 years and 11 months.

MATERIALS AND METHODS

Local research ethics board approval is not required for single case publications. Written consent was obtained from the patient's parents for autopsy and verbal consent obtained for case publication.

Genetic analysis was done by single gene testing of the *TUBB4A* gene at the Nemours Molecular Diagnostics Laboratory in Wilmington, Delaware, United States.

The brain was retrieved approximately 18 hours after death. The selected sections, all taken in the left hemisphere, were embedded in paraffin and stained with hematoxylin phloxin saffron (HPS). The following stains were used to characterize various features: cresyl violet, Luxol-periodic acid Schiff (PAS), Luxol-Bielschowski, PAS, and iron stain. Immunohistochemistry was carried out with a BOND-MAX automated system (Leica MicroSystems, Wetzlar, Germany) for glial fibrillary acidic protein (GFAP) (dilution: ready to use; Leica PA0026), neurofilament (NF) 70 (dilution: 1:1000, Dako M0762), and 200 (dilution: ready to use; Leica PA0371), Neu-N (dilution: ready to use; Chemicon MAB377; very sub-optimal reaction likely in view of the delay between death and brain fixation) and CD68 (dilution: ready to use; Leica PA0273). Tissue sections were subject to epitope retrieval using the Bond epitope retrieval solution (Leica) appropriate to the primary antibody. Primary antibody binding was detected using the Bond Polymer Refine Detection system (Leica) which is biotin-free. This system exposes tissue sections to primary antibody for 15 minutes, post-primary solution for 8 minutes, Bond polymer for 8 minutes, peroxide block for 5 minutes, 3,3-diaminobenzidine (DAB) chromogen for 10 minutes, and hematoxylin counter-stain for 7 minutes. A positive control was included on each slide.

RESULTS

Imaging

Initial MRI at 6 months of age showed ventriculomegaly secondary to decreased cerebral white matter volume, most prominent in the occipitoparietal regions (Fig. 1). There was also diffuse thinning of the corpus callosum and generalized lack of myelination of the cerebral white matter. Repeat MRI at 11 and 17 months old demonstrated no progression of myelination, and progressive atrophy of the caudate, putamen, cerebellum, cerebral hemispheres, and corpus callosum (Fig. 1). There was also a retro-cerebellar cystic structure that remained stable throughout. MR spectroscopy was normal. CT scan showed no evidence of intracranial calcifications.

Genotype

Our patient had a de novo heterozygous mutation c.533C>G (p.Thr178Arg) in exon 4 of the *TUBB4A* gene.

Neuropathological Examination

Gross Description

The brain weighed 716.5 grams (expected weight: 1204.2 ± 72.9 grams). The posterior fossa content weighed 47.5 grams (6.6%) and the cerebellum alone 35.5 grams (5%). The gyri showed mild generalized atrophy. The mammillary bodies were flattened. The optic nerves and chiasm were small and gray. The brainstem showed moderate atrophy with small cerebral peduncles and pyramids. The basis pontis was mildly flattened. The cerebellum was very small and firm. The cranial caudal thickness was significantly reduced, and the cisterna magna was very wide. The spinal cord was mildly thinned, but the nerve roots were normal.

The coronal sections of the cerebral hemispheres showed a severe ventriculomegaly, slightly worse on the left. The volume of the white matter was significantly reduced. The cerebral cortex appeared within normal limit, but the hippocampi were smaller than normal. Several structures were not clearly identified: caudate nuclei, putamina, claustrum, external, and extreme capsules, expanded perivascular spaces being present in these regions (Fig. 2A). Only the posterior limbs of the internal capsules were identified and were very atrophic. The mammillary bodies were atrophic. The corpus callosum was very atrophic; the fornices and the anterior commissure were thinner than normal (Fig. 2A). Transverse sections of the brainstem showed severe atrophy of the corticospinal tracts. The basis pontis was atrophic with a basis pontis/tegmentum ratio around 1. It was also very white in appearance, as were the inferior olivary nuclei. The superior and middle cerebellar peduncles were atrophic. The sections of the cerebellum showed generalized, severe atrophy of the cortex along with severe loss of the white matter. The dentate nuclei were hazy and white (Fig. 2B). The transversal sections of the spinal cord did not show definite changes.

Histological Description

The white matter of the cerebral and cerebellar hemispheres showed a generalized lack of myelin with only rare small slightly myelinated fields without any specific topography (Fig. 3A, B). The subcortical U-fibers were largely involved. There was severe loss of oligodendrocytes and severe reactive gliosis (Fig. 3A insert). The microglial reaction was mild and a few macrophages were present around some blood vessels, without intracytoplasmic myelin debris. Lymphocytic perivascular cuffing was rarely seen. Rare spheroids were also noted. Similar changes were noted in the optic tracts (Fig. 3C, D), corpus callosum and all white tracts of the cerebral hemispheres and brainstem and white matter throughout the cerebellum. In the spinal cord, severe changes were noted in the cortical spinal tracts and, to a lesser degree, in all the other descending tracts. The NF 70 and 200 showed a decrease in the number of axons in these structures.

In the neostriatum, equally in the putamen and caudate nucleus, there was a very severe atrophy (Fig. 4A) with loss of neurons (Fig. 4B), severe gliosis (Fig. 4B, insert), and atrophy of the striato-pallidal fibers. Large neurons were significantly

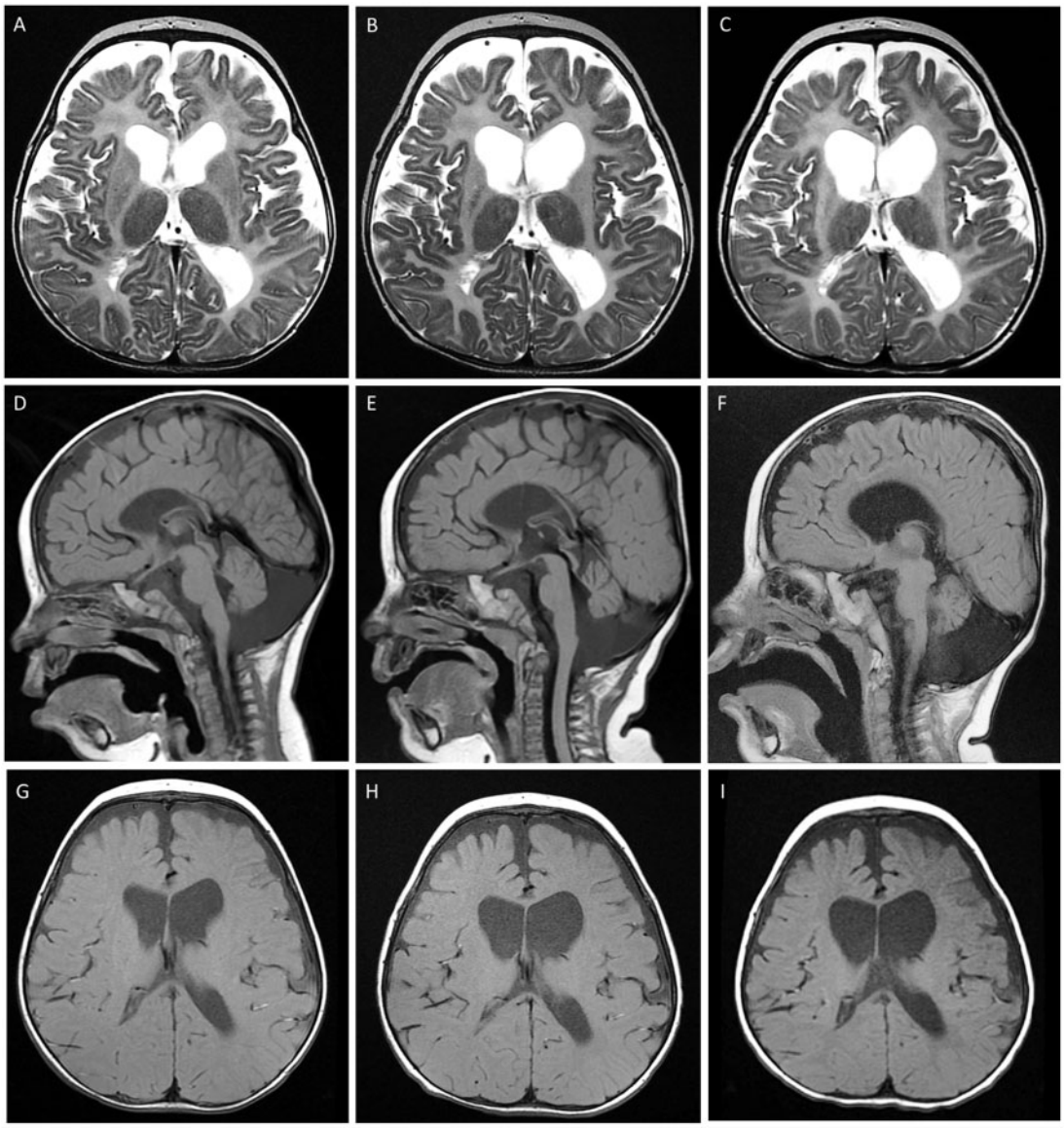

FIGURE 1. MRI images at 6 (**A**, **D**, **G**), 11 (**B**, **E**, **H**), and 17 **(C**, **F**, **I)** months of age. (**A–C)** Decreasing size of the caudate and putamen and enlargement of ventricles. Also evident is the lack of myelination, with the parieto-occipital regions more affected than anteriorly. (**D–F**) Progressive atrophy of the cerebellum and thin corpus callosum. (**G–I)** Lack of progression of myelination.

reduced in number (Fig. 4B). In the globus pallidus, there was mild to moderate loss of neurons, those present showing features of simple atrophy. Moderate neuronal loss was also noted in the thalamus. Moderate gliosis was noted in these structures and all other supratentorial neuronal structures. The basal forebrain had a normal neuronal population.

In the left insular region, on the temporal side, the neocortex showed features of focal cortical dysplasia with thickening and festooned interface with the underlying white matter (Fig. 4C). The molecular layer showed Chaslin's gliosis and a focal increase in neurons. There were rare hypertrophic neurons but no ballooned cells (Fig. 4D). The claustrum could not be identified at the level of the dysplasia. The underlying white matter showed an increased number of neurons, isolated or in clusters (Fig. 4E). These heterotopic neurons were predominantly seen in the subcortical region of the Sylvian region, thus under or near the dysplastic focus. The rest of the neocortex showed an uneven mild neuronal loss with a moderate transcortical reactive gliosis and a mild patchy spongiosis of the second cortical layer.

The hippocampus was smaller than normal (Fig. 5A). The dentate gyrus showed moderate dispersion with mild uneven loss of neurons (Fig. 5B). The CA4 sector showed a mild to moderate loss of neurons with moderate gliosis (Fig. 5C). The CA3 sector was also gliotic. The CA1 sector showed a very severe loss of neurons with dense gliosis, all ending

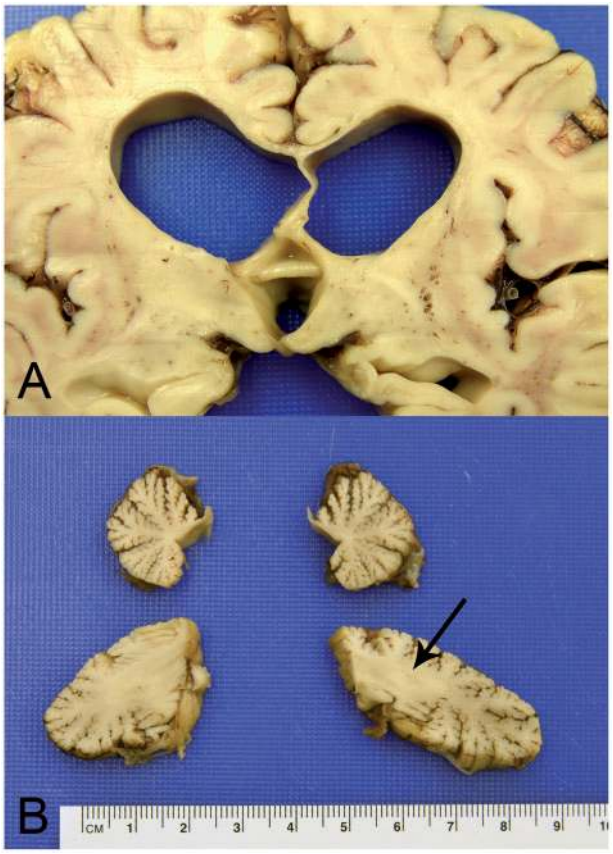

FIGURE 2. (**A**) Coronal section of the cerebral hemispheres showing enlargement of the cerebral ventricles slightly more severe on the left side, markedly reduced volume of the white matter, non-visualized or ill-defined deep gray structures and internal capsules, thin corpus callosum, fornices and anterior commissure and perivascular cystic enlargement. (**B**) Sagittal sections of the cerebellum showing a reduced volume and severe atrophy of the cortex, worse in the vermis (sections above), reduced volume of white matter and whitish appearance of the dentate nuclei (sections below, arrow).

abruptly with a relatively normal population in the subiculum (Fig. 5A). These changes were interpreted as consistent with hippocampal sclerosis.

In the brainstem, besides the changes in all the white matter tracts, there was moderate neuronal loss in the substantia nigra and red nuclei. The loss was somewhat milder in the periaqueductal gray matter, colliculi, pontine gray nuclei, tegmentum of the pons and medulla and inferior olivary nuclei (patchy). All these structures showed a severe reactive gliosis. Increased perivascular space was noted in the floor of the fourth ventricle in the pons.

The cerebellar neocortex showed a mild to moderate loss of Purkinje cells, more severe in the vermis than in the hemispheres. The internal granular layer was largely depleted of neurons (Fig. 6A). There was minimal dispersion of the Purkinje cells. Numerous dendritic swellings of various shapes (Fig. 6B), rare torpedoes and severe Bergman's gliosis were associated with the neuronal abnormalities. The dentate nucleus showed a mild neuronal loss but a severe gliosis. In the anterior gray horns of the spinal cord, there was no definite loss of neurons but there was a severe gliosis. The sampled peripheral nerves and skeletal muscles were normal.

The retro-cerebellar structure detected by diagnostic imaging was inferred to be an arachnoid cyst ruptured at time of brain resection; the sections of the cerebellum do not show any non-arachnoid tissue. The presence of this cyst may explain some of the flattening of the cerebellum.

DISCUSSION

The most common mutation responsible for H-ABC is c.745G>A (p.Asp249Asn) in exon 4 of the *TUBB4A* gene and is associated with a milder clinical phenotype than seen in our patient. Patients with the common mutation have a later age of onset, are usually able to walk and speak initially, and have milder growth restriction and degree of hypomyelination (2).

Miyatake et al (4) described a child with the same mutation c.533C>G (p.Thr178Arg) as our patient, with a very similar phenotype (infantile onset spastic quadriparesis and epilepsy). Curiel noted that patients with seizures were much younger at presentation (4 months ±12.1) (5). Similarly, Hamilton et al (2) described that non c745G>A mutations resulted in clinically more severe phenotypes, including an increased frequency of seizures (53% vs 12%). A literature review of *TUBB4A* mutations causing the H-ABC phenotype stated that 32/75 patients had epilepsy (6).

Our patient presented severely with associated findings such as cortical visual impairment, pathologically confirmed optic tracts and pathways atrophy and myelin involvement, and hypodontia, features less recognized as part of the H-ABC phenotype. Although hypodontia has been associated with other leukodystrophies, such as POLR3-related hypomyelination and oculodentodigital dysplasia, hypodontia has only recently been seen in one other patient with H-ABC (7). Our patient showed delayed teeth eruption with an altered order, however, she did not follow the typical 4 H pattern of molar eruption first, nor did she show the typical brittleness of ODDD. There are only a couple documented cases involving visual impairment. Our patient had a normal fundoscopic exam and was diagnosed clinically as having cortical visual impairment. Histologically, the optic nerves showed lack of myelin, severe gliosis and uneven loss of axons, findings not previously reported in H-ABC pathology.

Different mutations of the *TUBB4A* gene appear to preferentially affect different areas of the brain, and even different cell types within the brain, and thus result in differing clinical phenotypes. For example, clinical syndromes ranging from primary dystonia, to spastic diplegia, to isolated hypomyelination, to H-ABC, to infantile encephalopathy, have all been described secondary to *TUBB4A* mutations, with H-ABC being the only one demonstrated to affect both neurons and oligodendrocytes (5) and for this reason, is proposed to be considered a leuko-axonopathy (1). The c.533C>G (p.Thr178Arg) mutation is in the region where GTP binds with the β-tubulin, which is necessary for tubulin polymerization to occur (4), while the c.745G>A (p.Asp249Asn) mutation affects an amino acid that is important for the stability of assembled microtubules. αβ-Tubulin heterodimers assemble to form

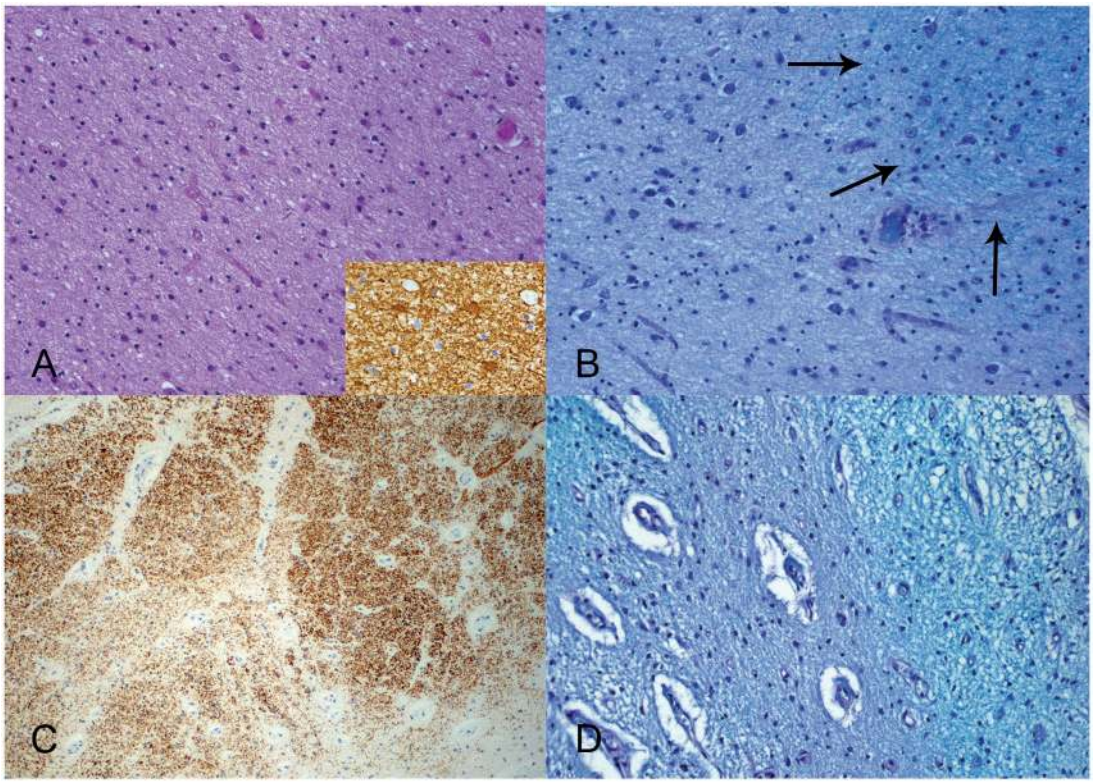

FIGURE 3. (**A**) White matter of the cerebral hemisphere with lack of myelin, reduced number of oligodendrocytes and (insert) reactive gliosis (HPS, 200×; insert GFAP, 400×). (**B**) Myelin stain of the white matter showing a rare focus of residual myelin in the upper right corner (arrows) (Luxol-PAS, 200×). (**C**) Optic nerve showing features of atrophy with enlarged perivascular spaces and predominantly central loss of NF-200-positive axons (NF200, 100×) (**D**) Optic nerve showing patchy demyelination (Luxol-PAS, 400×).

microtubules, which are essential for several functions including cell motility, mitosis, neuronal morphology, and intracellular transport, including the transport of myelin mRNAs and proteins (5,8,9). While microtubules are essential for all nucleated cells, the *TUBB4A* gene encodes a brain-specific β-tubulin that is expressed predominantly in the cerebellum, putamen, and white matter (10).

Previous neuropathological descriptions of H-ABC are limited to one patient with an unknown gene mutation (11) and 2 with the more common c.745G>A mutation (5). Our patient showed the previously documented cardinal features of H-ABC: atrophy of the cerebellum with neuronal loss predominant in the internal granular layer; atrophy of the putamen and hypomyelination resulting in significant volume loss with atrophy of the pyramidal tracts. However, our patient demonstrated findings beyond the severity and scope of the reported cases: atrophy of the caudate nucleus as severe as in the putamen; variable neuronal loss in several gray structures such as the globus pallidus, thalamus, and substantia nigra; severe reactive gliosis affecting the hypothalamus, subthalamic nucleus, and amygdala, the entire brainstem and spinal cord; and defect of myelin affecting essentially all the white matter tracts of the central nervous system, quite severe in the optic tracts and corpus callosum. Furthermore, an area of focal cortical dysplasia in the temporal versant of the Sylvian region and evidence of neuronal migration abnormalities were documented. If one associates the hippocampal changes consistent with hippocampal sclerosis, this combination may represent a type IIIa of the latest International League Against Epilepsy classification of focal cortical dysplasia (12).

As has been previously described in (5), different mutations in the *TUBB4A* gene can result in differing patterns of cell dysfunction. Our neuropathological findings thus suggest that the c.533C>G mutation confers a more severe morphological phenotype strengthening the experimental and pathological data linking these mutations to involvement of both neurons and myelin. The finding of an area of focal cortical dysplasia is not surprising given the dysfunction of tubulin. Other tubulinopathies have been responsible for a wide variety of brain malformations including cerebellar atrophy, lissencephaly, and polymicrogyria (6).

It remains to be seen if it is an isolated finding in our patient, if it is related to this specific mutation, or if it could happen with other mutations. Similarly, more morphological descriptions are needed to explain the hippocampal findings in the context of *TUBB4A* mutations presenting with epilepsy as part of their clinical evolution.

In summary, our patient demonstrates a severe clinical phenotype with features such as visual dysfunction that have been noted to occur but are not fully considered part of the

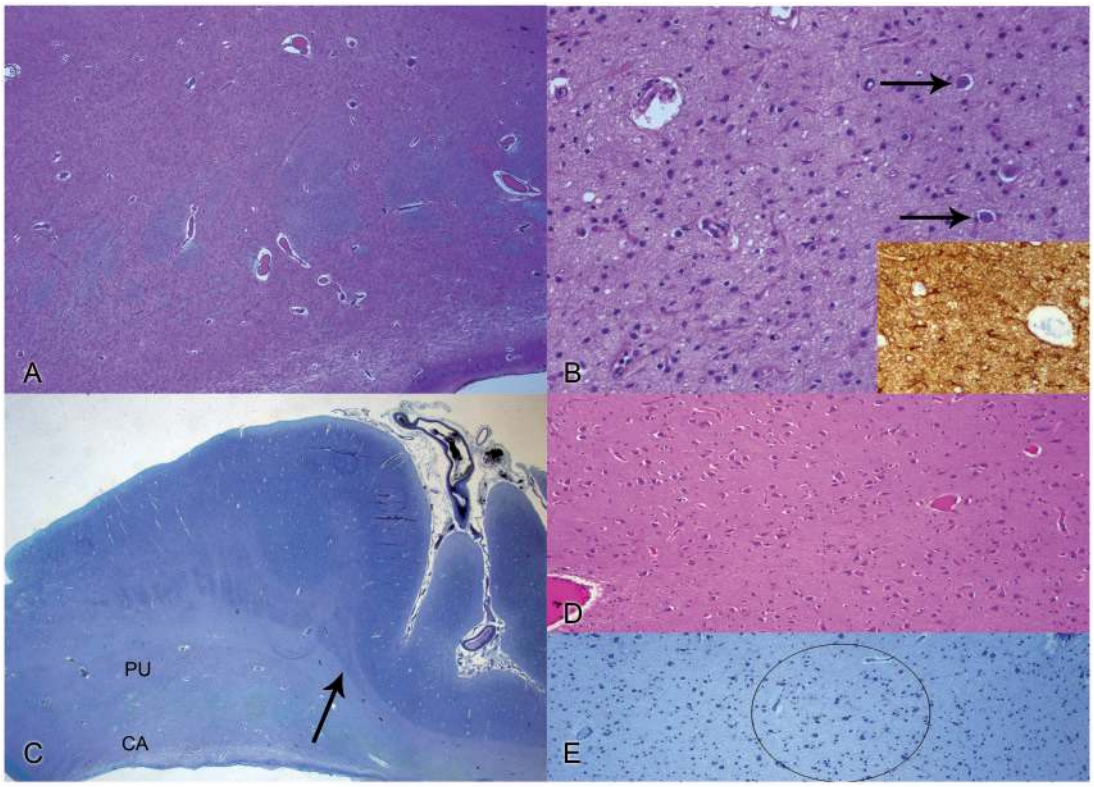

FIGURE 4. (**A**) Low-power view of the striatum showing equally severe atrophy of the caudate and putamen and a severe atrophy of the internal capsule (HPS, 20×). (**B**) Putamen with few residual large neurons (arrows) and (insert) severe gliosis (HPS, 200×; GFAP, 200×). (**C**) Cortex of inferior insular region showing focal cortical dysplasia, extending from the arrow to the left side of the photo, with thickened cortical ribbon and festooned interface with the underlying white matter (Luxol-PAS, 5×). (**D**) Higher-power view of the dysplastic focus with unlayered, disorganized neurons without dysmorphism or ballooned cells (HPS, 200×). (**E**) White matter underlying the focal cortical dysplasia with a loose cluster (circle) of heterotopic neurons (Luxol-PAS, 100×).

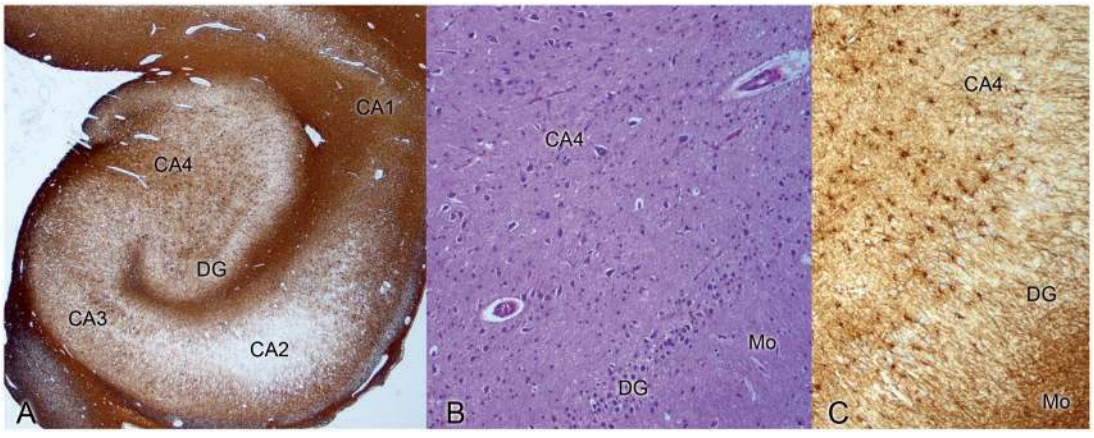

FIGURE 5. (**A**) Low-power view of the hippocampus confirming the gross impression of reduced volume with this magnification; this GFAP stain shows a dense gliosis of the CA1 sector, moderate gliosis of the CA4 sector extending into the CA3 sector and a relative sparing of the CA2 sector (20×). (**B**) Dentate gyrus of the hippocampus with uneven dispersion and neuronal loss; CA4 sector with neuronal loss and reactive gliosis (HPS, 200×). (**C**) GFAP stain showing the moderate gliosis involving the CA4 sector and dentate gyrus but severe in the molecular layer (GFAP, 200×) Labels: Mo, molecular layer of the dentate gyrus; DG, dentate gyrus; CA, cornu ammonis 1–4.

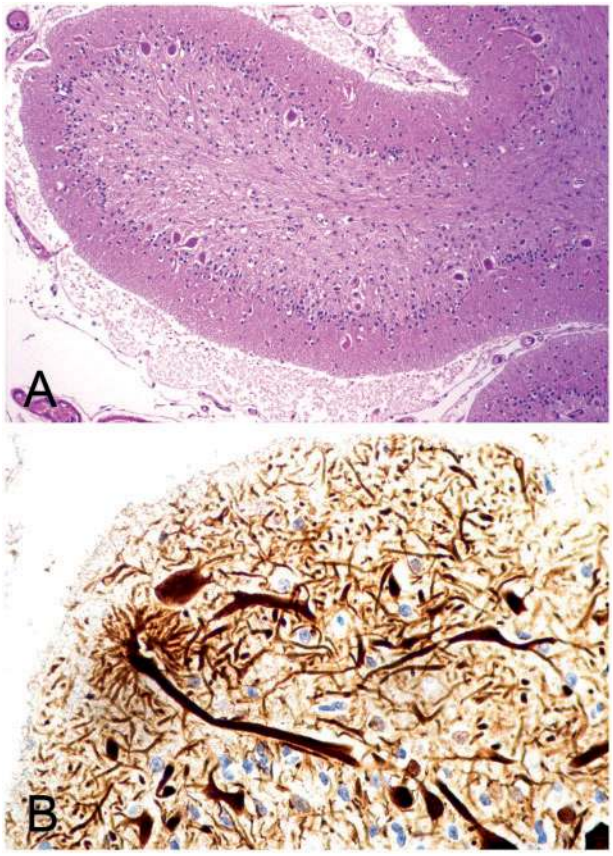

FIGURE 6. (**A**) Vermian cortex showing a moderate loss of Purkinje cells, a severe loss of neurons in the internal granular layer and a thinned molecular layer with occasional hypertrophic dendrites (HPS, 100×). (**B**) NF200 immunohistochemical reaction in the molecular layer showing very abnormal dendrites, in size and shape (200×).

H-ABC phenotypic spectrum. Hypodontia has been described only once previously, and tonic spasms have not been described in these patients previously. This provides an even greater variation to the signs and symptoms that neurologists must consider when presented with a patient with H-ABC. Morphologically, compared to previously reported cases, the changes are more severe and widespread in the white matter and tracts including the optic nerves, more severe in the caudate nucleus and involve other structures such as the thalamus, globus pallidus, and substantia nigra. This constellation of neuropathological findings, along with a focus of cortical dysplasia, provides similarities between *TUBB4A* and other tubulinopathies.

REFERENCES

1. Van der Knaap MS, Bugiani M. Leukodystrophies: A proposed classification system based on pathological changes and pathogenetic mechanisms. Acta Neuropathol 2017;134:351–82
2. Hamilton EM, Polder E, Vanderver A, et al. Hypomyelination with atrophy of the basal ganglia and cerebellum: Further delineation of the phenotype and genotype-phenotype correlation. Brain 2014;137: 1921–30
3. Van der Knaap MS, Naidu S, Pouwels PJW, et al. New syndrome characterized by hypomyelination with atrophy of the basal ganglia and cerebellum. AJNR Am J Neuroradiol 2002;23:1466–74
4. Miyatake S, Osaka H, Shiina M, et al. Expanding the phenotypic spectrum of *TUBB4A*-associated hypomyelinating leukoencephalopathies. Neurology 2014;82:2230–7
5. Curiel J, Bey GR, Takanohashi A, et al. *TUBB4A* mutations result in specific neuronal and oligodendrocytic defects that closely match clinically distinct phenotypes. Hum Mol Genet 2017;26:4506–18
6. Romaniello R, Arrigoni F, Bassi MT, et al. Mutations in α- and β-tubulin encoding genes: Implications in brain malformations. Brain Dev 2015; 37:273–80
7. Tonduti D, Aiello C, Renaldo F, et al. *TUBB4A*-related hypomyelinating leukodystrophy: New insights from a series of 12 patients. Eur J Paediatr Neurol 2016;20:323–30
8. Nogales E. A structural view of microtubule dynamics. Cell Mol Life Sci 1999;56:133–42
9. Nawrotek A, Knossow M, Gigant B. The determinants that govern microtubule assembly from the atomic structure of GTP-tubulin. J Mol Biol 2011;412:35–42
10. Online Mendelian Inheritance in Man [database online]. Baltimore, MD: McKusick-Nathans Institute of Genetic Medicine, Johns Hopkins University School of Medicine. Entry *602662 TUBULIN, BETA-4A; TUBB4A. Updated June 16, 2015.
11. Van der Knaap MS, Linnankivi T, Paetau A, et al. Hypomyelination with atrophy of the basal ganglia and cerebellum: Follow-up and pathology. Neurology 2007;69:166–71
12. Blümcke I, Thom M, Aronica E, et al. The clinico-pathological spectrum of focal cortical dysplasias: A consensus classification proposed by an ad hoc Task Force of the ILAE Diagnostic Methods Commission. Epilepsia 2011;52:158–74